Optical Spectra of Oxy- and Deoxyhemoglobin

William A. Eaton,*[1,2a] Louise Karle Hanson,[2a] P. J. Stephens,[2b] J. C. Sutherland,[2b] and J. B. R. Dunn[2b]

Contribution from the Laboratory of Chemical Physics, National Institute of Arthritis, Metabolism and Digestive Diseases, National Institutes of Health, Bethesda, Maryland 20014, and the Department of Chemistry, University of Southern California, Los Angeles, California 90007.
Received November 28, 1977

Abstract: The optical spectra of oxy- and deoxyhemoglobin are investigated over a wide frequency range using the techniques of polarized single crystal absorption spectroscopy and solution natural and magnetic circular dichroism. In addition to the porphyrin $\pi \rightarrow \pi^*$ transitions, seven transitions of oxyhemoglobin and four transitions of deoxyhemoglobin are characterized. Most of these transitions occur in the near-infrared spectral region. To make assignments extended Hückel calculations are carried out on the complex of iron-porphin with imidazole as a model chromophore for deoxyhemoglobin, with the addition of oxygen to obtain a model chromophore for oxyhemoglobin. Calculations are also carried out on the corresponding carbon monoxide complex to aid in the interpretation of the oxyhemoglobin spectra. Assignments are proposed for all of the transitions in terms of one-electron excitations between single configurations. Five of the seven bands of oxyhemoglobin are assigned to transitions into the lowest empty molecular orbital, which is delocalized over the FeO_2 unit. Three of the four bands of deoxyhemoglobin are assigned to porphyrin↔iron charge-transfer transitions. The remaining bands are interpreted as arising from d → d transitions of the iron.

In this paper we present a detailed experimental and theoretical investigation of the optical spectra of the heme complexes in oxy- and deoxyhemoglobin. The principal objectives of this study are to characterize experimentally as many electronic transitions as possible and to assign them to specific orbital promotions. Firm spectroscopic assignments are important, for the experimental parameters can then be used for testing theoretical descriptions of ground and excited state electronic structure in hemoglobin. The assignments are also required for interpreting spectral perturbations in terms of structural changes,[3a-c] and for understanding the mechanism of photolysis of oxy- and carbonmonoxyhemoglobin.[3d]

Our experimental approach has been to synthesize the results of optical absorption measurements that employ plane or circularly polarized light over a wide frequency range. The measurements include the polarized absorption of single crystals and the natural and magnetic circular dichroism of solutions (CD and MCD). From the single crystal spectra we obtain directions for the electric-dipole transition moments, while the CD and MCD spectra also depend on magnetic-dipole transition moments. At present the experimental information is limited to the "window" between about 4000 (2500 nm) and 33 000 cm^{-1} (300 nm). Transitions at lower frequencies are masked by solvent and protein vibrational absorption, while protein electronic absorption obscures heme transitions at higher frequencies. We present our experimental results in detail primarily for the near-infrared spectral region, since the visible and near-ultraviolet spectra using the three different techniques have been previously reported by us or by others. With the addition of the near-infrared spectroscopic data reported here, it is now possible to locate and characterize seven transitions in the optical spectra of oxyhemoglobin, in addition to the porphyrin $\pi \rightarrow \pi^*$ transitions. Four such transitions can be described for deoxyhemoglobin.

Our theoretical approach has been to use crystal field theory and the iterative extended Hückel molecular orbital method of Zerner, Gouterman, and Kobayashi to make the assignments.[4] For the extended Hückel calculations we have used the complex of iron-porphin with imidazole as a model chromophore for deoxyhemoglobin, with the addition of oxygen to obtain a model chromophore for oxyhemoglobin. Using the results of these calculations we attempt to assign the seven transitions of oxyhemoglobin and the four transitions of deoxyhemoglobin in terms of spin-allowed electronic promotions between single configurations. This is a difficult task for several reasons. A much larger number of transitions are predicted in the experimental frequency range than are observed. We have no good independent estimate of the reliability of the predicted frequencies, which appear to be in error by as much as 10 000 cm^{-1}. Finally, no absorption, MCD, or CD amplitudes have been calculated, so that our discussion of these must depend, in most cases, on semiquantitative or qualitative arguments. Nevertheless, we have been able to make reasonably convincing assignments of the observed transitions.

This study is part of a series of investigations on the interpretation of heme protein optical spectra using polarized light techniques. We have previously reported results of work on various complexes of myoglobin,[5] hemoglobin,[6] and cytochromes *c*,[7] *c'*,[8] and P-450.[9] A preliminary account of the present work on oxyhemoglobin has been reported elsewhere.[10]

Experimental Section

Concentrated solutions of horse and human hemoglobin were prepared by standard procedures.[11] Deoxygenation of solutions was carried out under nitrogen by the addition of excess sodium dithionite (Vine Chemicals Ltd., Widnes, Cheshire, England). All solution spectral measurements were carried out in 0.1 M potassium phosphate buffer, pH 7, at room temperature. For measurements at wavelengths longer than 1200 nm, the solutions were dialyzed against D_2O containing the same buffer. Crystallization of human deoxyhemoglobin A was carried out according to the method of Perutz,[11] except that sodium dithionite was used instead of ferrous citrate. Prior to spectral measurements the crystals were washed with a solution containing the same salt composition as the mother liquor (2.2 M ammonium sulfate, 0.3 M ammonium phosphate, 0.01 M sodium dithionite, pH 6.5).

Polarized single crystal absorption spectra were measured at room temperature with a microspectrophotometer described previously.[12] For measurements in the near-infrared to 1150 nm a tungsten source, Hamamatsu R196 photomultiplier tube (S-1 response), and a single ¼ m Ebert monochromator with 590 grooves/mm grating blazed at 1000 nm (Jarrell-Ash) were employed. The space group of human deoxyhemoglobin A crystals is $P2_1$ with two molecules (eight hemes) per unit cell.[11,13] Spectra were measured on the (010) crystal face with light polarized parallel to either the *a* or *c** axes. These axes had been previously identified from a combination of x-ray photography and optical measurements in the visible and near-ultraviolet spectral regions.[14] In the present study the *a* and *c** axes were found to remain the principal optical directions to within ±3° throughout the near-

0002-7863/78/1500-4991$01.00/0

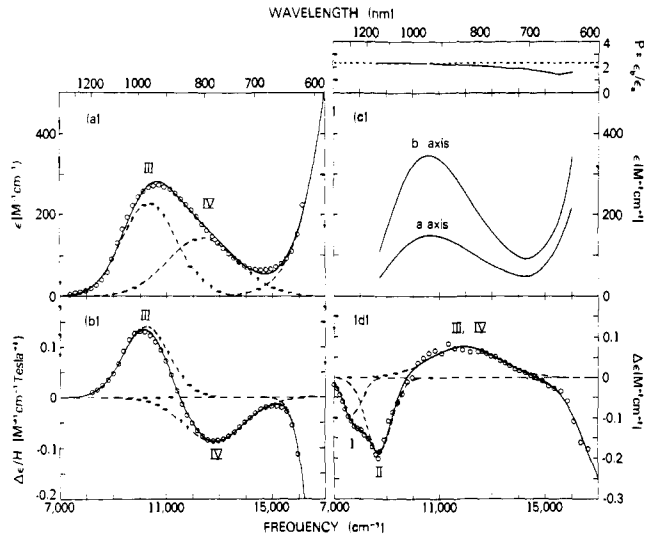

Figure 1. Near-infrared optical spectra of oxyhemoglobin at room temperature. All spectra were measured in H_2O, except the CD, which was measured in D_2O. (a) Solution absorption spectrum of horse oxyhemoglobin. (b) Solution MCD of horse oxyhemoglobin. (c) Polarized single crystal absorption spectrum of horse oxyhemoglobin on the (001) crystal face with the electric vector of the plane-polarized light parallel to the *a* and *b* crystal axes. The *b*/*a* polarization ratio is plotted above the spectra. The horizontal dashed line is drawn at the polarization ratio of 2.27 measured for the *x*,*y*-polarized Soret band.[6a,21b] This crystal spectrum was previously reported by Makinen and Eaton.[6a] (d) Solution CD of human oxyhemoglobin A. In (a), (b), and (d) the circles are the experimental points, the dashed curves are the Gaussian components obtained from a least-squares fit to the experimental points, and the solid curve is the sum of the Gaussian components. The parameters of the Gaussian bands I–IV are given in Table I. The position, width, and amplitude parameters used to fit the tail of the Q_0 band were 20 600, 2700, 3000 in (a); 17 600, 1000, −1.3 in (b); and 17 900, 1600, −0.34 in (d).

infrared region by measuring the angular dependence of absorption and of the light intensity transmitted through crossed polarizers.

Solution absorption measurements were made with either a Cary 14 or 17 recording spectrophotometer. Near-infrared CD and MCD spectra were measured with an instrument previously described.[15] For MCD measurements magnetic fields of about 40 kG were provided by a superconducting magnet. In the visible spectral region CD measurements were made with a Cary 6001 or 61 spectrometer. CD and MCD data are reported in terms of $\Delta\epsilon$; in the case of MCD $\Delta\epsilon$ is normalized to a field of +10 kG (1 T).

Results

A. Oxyhemoglobin Spectra. Figure 1 shows the near-infrared solution absorption, CD, and MCD spectra of oxyhemoglobin, and the polarized single crystal absorption spectrum measured by Makinen and Eaton.[6a] The near-infrared MCD spectrum was reported earlier,[16] and agrees satisfactorily with the one displayed by Sutherland et al.[17] Above 15 000 cm^{-1} MCD and absorption in Figure I arises from the much more intense porphyrin Q bands. Quantitative analysis of the spectra was carried out by fitting the experimental curves to a sum of Gaussian bands using a least-squares curve-fitting procedure described by Knott and co-workers.[18] Our strategy in the curve fitting was to use the minimum number of Gaussian components that would produce a physically reasonable resolution of the data. The peak position, peak amplitude, and half-bandwidth for each Gaussian component are given in Table I.

The solution absorption spectrum is not very informative. Only a single broad band is observed that peaks at about 10 800 cm^{-1} (925 nm). If we look at the results of the polarized light experiments, however, there is evidence for four bands. These are labeled I–IV in Figure 1 and Table I, in order of increasing frequency.

The CD spectrum shows two negative bands at 7700 and 8700 cm^{-1}, labeled bands I and II. There is no evidence for corresponding absorption bands, indicating that these transitions have very large anisotropy factors. The CD anisotropy factor for band I is at least 10^{-2}, which is diagnostic of a magnetic-dipole allowed transition. No MCD corresponding to bands I and II is observed.

Bands III and IV are contained in the broad 10 800-cm^{-1} absorption band. The average polarization ratio through this band is very close to, but with significant variation from, the *x*,*y*-polarized value for the Soret band. The MCD shows large positive and negative extrema characteristic of an *A* term or of overlapping *B* terms arising from interacting near-degenerate excited states. Curve fitting to the MCD, assuming overlapping *B* terms, produces bands with peaks at 10 200 and 12 800 cm^{-1}, labeled bands III and IV. The areas under these MCD bands are the same to within 20%. In order to calculate MCD anisotropy factors, the solution absorption spectrum was then fit with two Gaussian bands. It was possible to obtain peak positions and bandwidths which are very similar to the values obtained for the corresponding MCD bands. The broad positive CD associated with the 10 800-cm^{-1} absorption is assumed to arise from both bands III and IV, and no resolution of the CD was attempted in the curve-fitting procedure.

Absorption measurements to 4000 cm^{-1} and CD measurements to 5500 cm^{-1} in D_2O solutions revealed no additional near-infrared electronic transitions.

Figures 2b and 2a show the solution absorption and CD spectra of oxyhemoglobin in the visible spectral region. The CD spectrum is not significantly different from previously reported spectra,[19] except for small differences that can be attributed to experimental uncertainties in establishing a correct baseline. Resolution of the spectrum into Gaussian components shows that there are two positive CD bands associated with the porphyrin Q_0 and Q_v bands at 17 300 and 18 500 cm^{-1}, and two additional broader bands at 18 400 and 20 900 cm^{-1}, labeled V and VI.[20] The parameters for these bands are summarized in Table II.

Also shown in Figure 2b is the *z*-polarized spectrum, calculated from the single crystal data of Makinen and Eaton,[6a] assuming that the intensity at each frequency is a linear combination of *z*-polarized and *x*,*y*-polarized intensity. This spectrum reveals a broad band at about 22 000 cm^{-1} (ϵ 1000 M^{-1} cm^{-1}, $\nu_{1/2}$ = 3000 cm^{-1}, f = 0.022); a second, more intense *z*-polarized band was found by Makinen and Eaton at about 31 000 cm^{-1} (ϵ 4400 M^{-1} cm^{-1}, $\nu_{1/2}$ = 4600 cm^{-1}, f = 0.15).[6a,10] We label these *z*-polarized bands VI and VII, associating the 22 000-cm^{-1} *z*-polarized absorption band with band VI of the CD spectrum.

In the interpretation of the oxyhemoglobin spectrum, comparison with the spectrum of carbonmonoxyhemoglobin is of considerable value. Makinen and Eaton found no *z*-polarized bands in their single-crystal study of the carbon monoxide complex.[6a] Figures 2d and 2c show the solution absorption and CD spectra of the carbon monoxide complex in the visible region.[19] An important feature of the CD spectrum is the very weak negative extremum at 15 200 cm^{-1} ($\Delta\epsilon$ −0.05 M^{-1} cm^{-1}), since it is the lowest observed electronic state of carbonmonoxyhemoglobin. The CD spectrum at higher frequencies is complex, but can be satisfactorily resolved into Gaussian components. The analysis in Figure 2c is based on the assumption that the CD spectrum consists of a broad positive CD band centered at 17 850 cm^{-1} superimposed on a series of relatively sharper bands. The four sharpest bands are readily associated with the porphyrin Q absorption bands. Both the *x* and *y* components of the degenerate Q_0 state are observed at 17 500 and 17 800 cm^{-1}, almost symmetrically positioned about the center of the Q_0 absorption band at 17 600 cm^{-1}. The CD band at 18 600 cm^{-1} corresponds to the Q_v

Table I. Near-Infrared Spectral Data for Oxyhemoglobin[a]

band	I	II	III	IV
ABS	*b*	*b*	10 400	12 400
ν_-, cm^{-1} MCD	*b*	*b*	10 200	12 800
CD	7700	8700	11 900	
ABS	*b*	*b*	1460	1850
$\nu_{1/2}$, cm^{-1} [c] MCD	*b*	*b*	1240	1610
CD	500	690	1800	
ϵ, $M^{-1}\,cm^{-1}$	(<10)[f]	(<50)[f]	230	145
$\Delta\epsilon$, $M^{-1}\,cm^{-1}\,T^{-1}$	*b*	*b*	0.141	−0.088
$\Delta\epsilon$, $M^{-1}\,cm^{-1}$	−0.094	−0.185	0.077	
f[d]	$(<4\times10^{-5})$[f]	$(<3\times10^{-4})$[f]	2.6×10^{-3}	2.1×10^{-3}
g(MCD)[e]	*b*	*b*	5.2×10^{-4}	5.3×10^{-4}
g(CD)[e]	$(>10^{-2})$[f]	$(>4\times10^{-3})$[f]	2.3×10^{-4}[g]	
polarization	*b*	*b*	*x,y*	

[a] These are the parameters obtained from fitting the spectra to a sum of Gaussian bands, as shown in Figure 1. [b] No distinct absorption or MCD bands are observed in this region. [c] This is the half-bandwidth at $1/e$ of the maximum amplitude, i.e., ϵ or $\Delta\epsilon$. [d] The oscillator strength is defined as $4.32\times10^{-9}\int\epsilon\,d\nu$, where the integral for a Gaussian band is $\sqrt{\pi}\epsilon\nu_{1/2}$. [e] The anisotropy factors are calculated as the ratio of the CD or MCD to absorption band areas. [f] Since no distinct absorption bands are observed, these are upper limits for the peak extinction coefficients and oscillator strengths. In calculating the upper limits for the oscillator strengths and lower limits for the CD anisotropy factors the CD bandwidths were used for the absorption band areas. [g] This anisotropy factor is the ratio of the area of the single CD band at 11 900 cm^{-1} to the sum of the absorption band areas for bands III and IV.

Table II. CD Data for Oxy- and Carbonmonoxyhemoglobin in Visible Spectral Region[a]

band	ν_-, cm^{-1}	$\Delta\epsilon$, $M^{-1}\,cm^{-1}$	$\nu_{1/2}$, cm^{-1}
	Oxyhemoglobin		
Q_0	17 300	3.20	310
Q_v	18 200	1.90	710
V	18 400	−0.83	1690
VI	20 900	1.37	1510
	Carbonmonoxyhemoglobin		
I	16 000	−0.4	920
Q_{0x}	17 500	−1.99	260
Q_{0y}	17 800	1.08	240
II	17 850	2.13	1570
Q_v	18 600	0.35	450
$Q_{v'}$	19 550	0.62	570

[a] These are the parameters obtained from fitting the spectra to a sum of Gaussian bands as shown in Figures 2a and 2c.

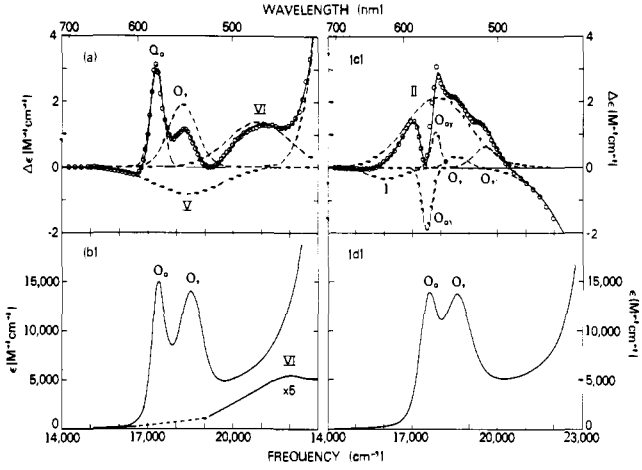

Figure 2. Visible solution absorption and CD spectra of oxy- and carbonmonoxyhemoglobin at room temperature. (a) CD spectrum of human oxyhemoglobin. (b) Solution absorption spectrum of human oxyhemoglobin and *z*-polarized spectrum calculated from the single crystal data of Makinen and Eaton[6a] for horse oxyhemoglobin. (c) CD spectrum of human carbon monoxyhemoglobin. (d) Solution absorption spectrum of human carbon monoxyhemoglobin. In (a) and (c) the circles are the experimental points, the dashed curves are the Gaussian components obtained from a least-squares fit to the experimental points, and the solid curve is the sum of the Gaussian components. The position, width, and amplitude parameters used to fit the tail of the Soret (B) CD band were 24 050, 1140, and 11.5 in (a); and 25 100, 2550, and −6.74 in (c).

absorption band at the same frequency, while the CD band at 19 600 cm^{-1} has the correct frequency separation to be a vibrational overtone, and is therefore labeled $Q_{v'}$. Thus only the negative CD band at 16 000 cm^{-1} and the positive CD band at 17 850 cm^{-1} cannot be ascribed to porphyrin $\pi\rightarrow\pi^*$ transitions. We label these bands I and II.

B. Deoxyhemoglobin Spectra. Figure 3 shows the near-infrared solution absorption, CD, and MCD spectra and the polarized single crystal absorption spectra of deoxyhemoglobin. The spectra have been resolved into Gaussian components, and the parameters are given in Table III for the solution spectra and in Table IV for the crystal spectra. The resolution of the MCD spectrum was carried out under the assumption that only *B* and *C* terms were present. A satisfactory resolution of all of the spectra with four bands of very similar peak positions and bandwidths was obtained despite the significant contribution to the absorption spectra from the tail of the broad porphyrin Q band. The four bands are labeled I–IV in Figure 3 and in Tables III and IV.

The bands are all of low intensity with oscillator strengths not exceeding 10^{-3}. Bands III and IV exhibit very large MCD anisotropy factors. Since the ground state of deoxyhemoglobin is paramagnetic, all four MCD bands could arise from either *B* or *C* terms, or from a combination of the two. In the absence of data on the temperature dependence of the MCD, we cannot separate the *B* and *C* term contributions.

Table IV gives a comparison of the observed crystal extinction coefficients and polarization ratios with those predicted from the crystal structure assuming pure *z* or pure *x,y* polarization. The orientations of the hemes used in these calculations are given in Table V. Both the crystal extinction coefficients and polarization ratios are consistent with almost pure *z* polarization for band I. Comparison of the results for band II indicates that it is mostly *z* polarized. Considering the uncertainties in obtaining accurate parameters from the curve-fitting procedure, we estimate that band II contains from 25 to 50% *x,y* polarization. Bands III and IV are polarized nearly parallel to the heme plane, but the data in Table IV for these bands suggest that there is unequal *x*- and *y*-polarized

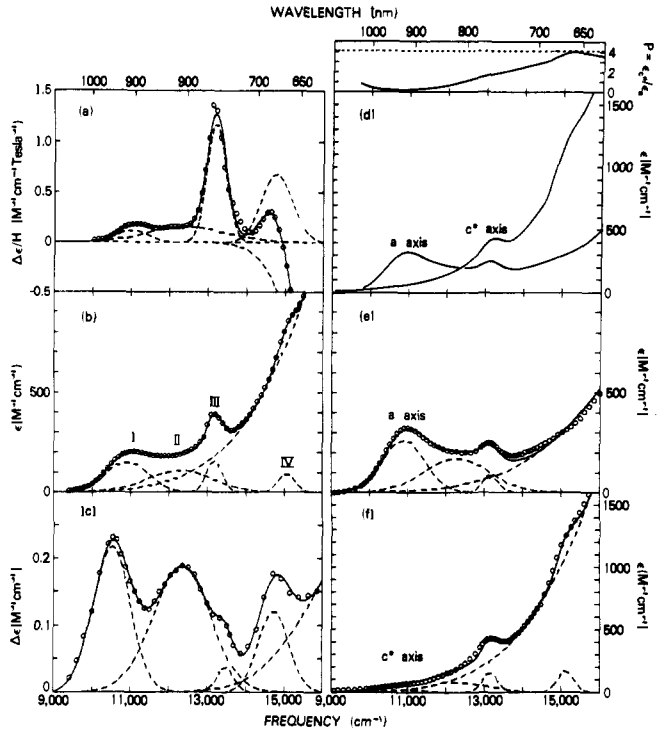

Figure 3. Near-infrared optical spectra of deoxyhemoglobin in H_2O at room temperature. (a) Solution MCD of horse deoxyhemoglobin. (b) Solution absorption spectrum of horse deoxyhemoglobin. (c) Solution CD spectrum of horse deoxyhemoglobin. (d) Polarized single crystal absorption spectrum of human deoxyhemoglobin A on the (010) crystal face with the electric vector of the plane polarized light parallel to the a and c^* axes. The c^*/a polarization ratio is plotted above the spectra. The horizontal dashed line is drawn at the polarization ratio of 4.0 measured by Hofrichter et al. for the x,y-polarized Soret band.[14] Crystal extinction coefficients are based on the optical density at 475 nm for the a-axis spectrum, using an extinction coefficient of 1230 M^{-1} cm^{-1} for ϵ_a. The c^*/a polarization ratio at this wavelength was measured to be 3.5, very close to the x,y-polarized value of 4.0 for the Soret band. This permitted the calculation of ϵ_a at 475 nm from the solution extinction coefficient (3500 M^{-1} cm^{-1}; E. Antonini and M. Brunori, "Hemoglobin and Myoglobin in Their Reactions with Ligands", North-Holland Publishing Co., Amsterdam, 1971, p 18) using the relation for an x,y-polarized transition given in the footnote to Table IV. This indirect procedure for obtaining crystal extinction coefficients was necessary because it was not possible to obtain accurate crystal thicknesses. It should introduce an error of less than 20%, however, and should therefore not influence any of the conclusions concerning band polarizations. In (a), (b), (c), (e), and (f) the circles are experimental points, the dashed curves are the Gaussian components obtained from a least-squares fit to the experimental points, and the solid curve is the sum of the Gaussian components. The parameters of the Gaussian bands I-IV are given in Tables III and IV. The position, width, and amplitude parameters used to fit the tail of the Q bands were 16 400, 1300, −2.4 in (a); 19 800, 3900, 3300 in (b); 17 200, 2000, 0.23 in (c); 21 700, 4600, 2400 in (e); and 21 700, 4600, 8200 in (f).

intensity. A preliminary crystal study on bands I-III of horse deoxyhemoglobin modified with bis(N-maleimidomethyl) ether[21] is consistent with the conclusions reached above.

Absorption measurements to 4000 cm^{-1} and CD measurements to 5500 cm^{-1} in D_2O solutions showed no additional near-infrared electronic transitions.

C. Theoretical Estimates of Carbonmonoxy- and Oxyhemoglobin Transition Frequencies. Until recently theoretical studies on the electronic structure of oxyhemoglobin have been hampered by the absence of definitive information on the geometry of the iron-oxygen bond. The difference Fourier x-ray diffraction study of oxymyoglobin by Watson and Nobbs favored a bent Fe-O-O configuration, as originally suggested by Pauling, but the oxygen molecule was not sufficiently resolved to rule out alternative structures.[22,23] The question appears to have been settled now by the determination of the

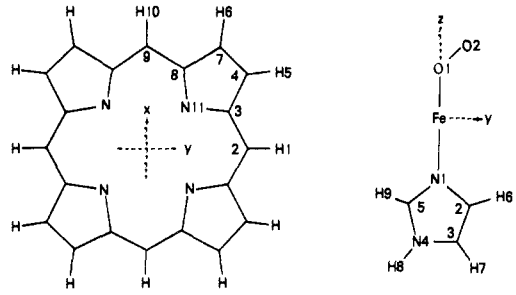

Figure 4. Structure of oxyheme complex used as model chromophore for oxyhemoglobin in extended Hückel calculations. Notice that the x and y axes are rotated 45° to those usually employed in ligand field theory.

x-ray structure of the "picket fence" iron-porphyrin complex of N-methylimidazole and oxygen by Collman and co-workers.[24] They found a Pauling-type structure with an Fe-O-O bond angle of 126°. The close correspondence of the O-O vibrational stretching frequencies in this model compound[25] and in oxyhemoglobin[26] indicates a similar bonding in oxyhemoglobin.

As a model chromophore for oxyhemoglobin we employed the neutral complex of iron, a square-symmetric porphin, imidazole, and oxygen shown in Figure 4. In the x-ray structure by Collman et al. two orientations of the oxygen molecule were found: in one the Fe-O-O plane is nearly parallel to the imidazole plane, and in the other the two planes are approximately perpendicular. Also the projection of the imidazole plane is closer to methine carbons than to pyrrole nitrogens. In order to maximize the symmetry of the complex, we used a structure in which the Fe-O-O and imidazole are coplanar, with their projection passing through opposite methine carbons. This molecule possesses a single plane of symmetry (point group C_s), which is taken as the yz plane (see Figure 4). The atomic coordinates for the model chromophore in Figure 4 are given in Table VI.

We carried out iterative extended Hückel calculations on this model chromophore using the method developed by Zerner, Gouterman, and Kobayashi.[4] Their calculations were confined to heme complexes with at least C_{2v} symmetry, so that the oxygen complex in Figure 4 could not have been used at that time. Since then Gouterman and co-workers have developed a computer program which permits calculations on heme complexes with no elements of symmetry. This program was kindly supplied to us by Professor Gouterman. It is described in detail in the paper by Schaffer et al.[27] Included in the calculations are the 1s orbital of hydrogen, the 2s and 2p orbitals of carbon, nitrogen, and oxygen, and the 3d, 4s, and 4p orbitals of iron. There are then 149 atomic orbitals and 158 electrons in our model chromophore. The parameters used in the calculations were the same as those given by Zerner et al.[4]

The energies of the resulting 149 molecular orbitals span the range −35 to +82 eV. Since we assume that the observed optical spectra of oxyhemoglobin arise from promotions involving the high-lying filled molecular orbitals and the low-lying empty molecular orbitals, we will generally need to consider only a small fraction of the total number of molecular orbitals. The molecular orbital energies are shown in Figure 5, together with the results for a carbon monoxide and deoxyheme complex discussed below. Notice that with the coordinate system used here (Figure 4), the d orbitals conventionally labeled $d_{x^2-y^2}$ and d_{xy} become relabeled d_{xy} and $d_{x^2-y^2}$, respectively; as a result, $d_{x^2-y^2}$ is lower in energy and is nonbonding, and d_{xy} is antibonding.

The most important feature in the orbital structure of the oxyheme complex is the strong interaction between the d_{xz} and d_{yz} iron orbitals and the orbitals that derive from the degenerate π_g orbitals of the free oxygen molecule. This interaction

Table III. Near-Infrared Solution Data for Deoxyhemoglobin[a]

band	I	II	III	IV
ν, cm^{-1}				
ABS	10 900	12 250	13 200	15 050
MCD	11 000	12 400	13 200	14 800
CD	10 500	12 350	13 500	14 750
$\nu_{1/2}$, cm^{-1}				
ABS	770	1200	290	310
MCD	550	1400	350	560
CD	690	1050	300	560
ϵ, M^{-1} cm^{-1}	155	110	150	90
$\Delta\epsilon$, M^{-1} cm^{-1} T^{-1}	0.12	0.16	1.18	0.7
$\Delta\epsilon$, M^{-1} cm^{-1}	0.22	0.19	0.04	0.12
f	9.1×10^{-4}	1.0×10^{-3}	3.3×10^{-4}	2×10^{-4}
g(MCD)[b]	5.5×10^{-4}	1.7×10^{-3}	9.5×10^{-3}	1.4×10^{-2}
g(CD)[b]	1.0×10^{-3}	1.5×10^{-3}	3×10^{-4}	2×10^{-3}

[a] These are the parameters obtained from fitting the spectra to a sum of Gaussian bands, as shown in Figure 2. See footnotes to Table I. [b] The anisotropy factors are defined as the ratio of CD or MCD to absorption band areas.

Table IV. Near-Infrared Deoxyhemoglobin Single Crystal Data[a]

band	I	II	III	IV
ν, cm^{-1}	10 900	12 250	13 200	15 150
$\nu_{1/2}$, cm^{-1}	770	1200	290	310
ϵ_c*, M^{-1} cm^{-1}	20	80	150	160
ϵ_c*(z)	5	3	5	3
ϵ_c*(x,y)	230	160	220	130
ϵ_a, M^{-1} cm^{-1}	265	170	85	0
$\epsilon_a(z)$	355	250	350	200
$\epsilon_a(x,y)$	55	40	55	30
$P = \epsilon_{c^*}/\epsilon_a$	0.08	0.5	1.8	>5
$P(z)$	0.013	0.013	0.013	0.013
$P(x,y)$	4.2	4.2	4.2	4.2
polarization	z	mostly z	in-plane	in-plane

[a] These are the parameters obtained from fitting the spectra to a sum of Gaussian bands as shown in Figure 3. See footnotes to Table I. In fitting the crystal spectra the c^* and a axis spectra were considered to have the same bandwidths and peak positions. The bandwidths were also constrained to have the same values as those found in fitting the solution absorption spectrum. The theoretical crystal extinction coefficients, $\epsilon_{c^*}(z)$, $\epsilon_{c^*}(x,y)$, $\epsilon_a(z)$, $\epsilon_a(x,y)$, and theoretical polarization ratios, $P(z)$, $P(x,y)$, are calculated from the relations $\epsilon_i(z) = \frac{3}{8}\epsilon \Sigma_{4\ \text{hemes}} \cos^2 zi$ and $\epsilon_i(x,y) = \frac{3}{4}\epsilon \Sigma_{4\ \text{hemes}} \sin^2 zi$ ($i = c^*, a$), which are derived from straightforward geometric considerations: J. Hofrichter and W. A. Eaton, *Annu. Rev. Biophys. Bioeng.*, **5**, 511-560 (1976). The solution extinction coefficients, ϵ, are taken from Table III, and the direction cosines for the heme normals are given in Table V.

Table V. Squared Direction Cosines of Heme Normal Relative to a, b, c^* Crystal Axes for Human Deoxyhemoglobin A[a]

	$\cos^2 za$	$\cos^2 zb$	$\cos^2 zc^*$
$\alpha 1$	0.5859	0.4090	0.0051
$\alpha 2$	0.8497	0.1243	0.0260
$\beta 1$	0.9292	0.0702	0.0006
$\beta 2$	0.7011	0.2896	0.0087

[a] The direction cosines were obtained from a Diamond real space refinement of the 2.8 Å crystal structure data as of April 1973, and were kindly given to us by Dr. A. D. McLachlan of the MRC Laboratory of Molecular Biology, Cambridge, England.

Table VI. Atomic Coordinates of Heme Complexes Used in Extended Hückel Calculations (Å)

molecule	atom	x	y	z
porphin[a]	H1	0.0	4.536	0.0
	C2	0.0	3.456	0.0
	C3	1.231	2.783	0.0
	C4	2.500	3.463	0.0
	H5	2.658	4.531	0.0
	H6	4.531	2.658	0.0
	C7	3.463	2.500	0.0
	C8	2.783	1.231	0.0
	C9	3.456	0.0	0.0
	H10	4.536	0.0	0.0
	N11	1.421	1.421	0.0
imidazole[b]	N1	0.0	0.0	2.060[e]
	C2	0.0	1.095	2.885
	C3	0.0	0.652	4.172
	N4	0.0	−0.708	4.148
	C5	0.0	−1.063	2.861
	H6	0.0	2.127	2.570
	H7	0.0	1.272	5.057
	H8	0.0	−1.370	5.001
	H9	0.0	−2.086	2.513
oxygen[c]	O1	0.0	0.0	−1.750
	O2	0.0	0.900	−2.620
carbon monoxide[d]	C	0.0	0.0	−1.750
	O	0.0	0.0	−2.870
iron	Fe(CO,O_2)	0.0	0.0	0.0
	Fe(deoxy)	0.0	0.0	0.620[f]

[a] Figure 4 shows the coordinate system. Since a square-symmetric porphin is used, only coordinates for a quarter-molecule are given. The porphin coordinates are the same as those used by Zerner et al.,[4] except that the pyrrole nitrogen is 2.01 Å from the molecular center instead of 2.05 Å. [b] The imidazole coordinates were obtained by averaging the results from four different crystal structures (S. Martinez-Carrera, *Acta Crystallogr.*, **20**, 783-789 (1966); J. Donohue, L. R. Lavine, and J. S. Rollett, *ibid.*, **9**, 655-662 (1956); J. W. Lauher and J. A. Ibers, *J. Am. Chem. Soc.*, **96**, 4447-4452 (1974); D. M. Collins, R. Countryman, and J. L. Hoard, *ibid.*, **94**, 2066-2072 (1972)), and imposing the constraint that the imidazole be planar. The imidazole coordinates in this table were used in the extended Hückel calculations on the oxygen and carbon monoxide complexes. For the deoxyheme calculation the imidazole was displaced 0.72 Å along the z axis in order to produce the 2.16 Å Fe-N1 distance reported by Hoard and Scheidt; J. L. Hoard and W. R. Scheidt, *Proc. Natl. Acad. Sci. U.S.A.*, **70**, 3919-3922 (1973). [c] From ref 24. [d] From S. M. Peng and J. A. Ibers, *J. Am. Chem. Soc.*, **98**, 8032-8036 (1976). [e] From ref 24. [f] This is the iron displacement reported by Fermi from the human deoxyhemoglobin A crystal structure; G. Fermi, *J. Mol. Biol.*, **97**, 237-256 (1975).

produces four closely spaced molecular orbitals that are composed mainly of iron d and oxygen π_g orbitals. The most important orbital for interpretation of the optical spectra is the empty mixed iron-oxygen molecular orbital that is only 0.24 eV above the top-filled molecular orbital. A lowest empty molecular orbital that is a mixture of iron d and oxygen π_g is a consistent feature of extended Hückel calculations carried out by Gouterman,[28] Loew,[29] and co-workers using a variety of Fe-O-O geometries. We have found that independent variation of the oxygen and imidazole orientations, with fixed Fe-O-O and Fe-N(imidazole) bond lengths and with a fixed Fe-O-O bond angle, affects the orbital energies by less than a few hundredths of an eV.

A comparison of oxy- and carbonmonoxyhemoglobin spectra is a useful aid for interpreting the more complex oxyhemoglobin spectra. We therefore carried out extended Hückel calculations on a model carbon monoxide chromophore. There is still some question concerning the detailed geometry of the Fe-C-O moiety in the carbon monoxide complexes of hemo-

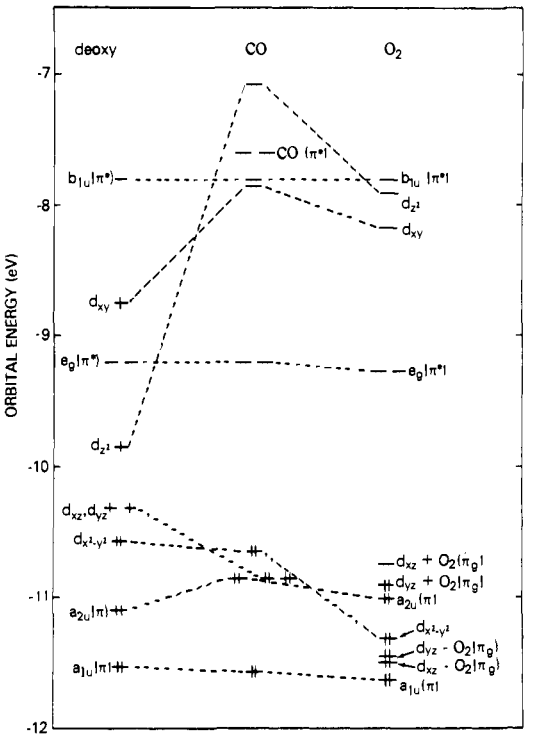

Figure 5. Extended Hückel orbital energies for deoxy-, carbonmonoxy-, and oxyheme complexes. Only the major contributors to each orbital are indicated. No imidazole orbitals lie between −7 and −12 eV. The highest filled imidazole orbital is at −12.72, −12.38, and −12.46 eV in the deoxy, carbonmonoxy, and oxy complexes, respectively, while the lowest empty imidazole orbital is at −6.39, −6.73, and −6.81 eV. Coefficients of the atomic orbitals for the oxygen complex were given by eaton et al.[10] Notice that the plus and minus signs in the mixed iron-oxygen orbitals are opposite to those expected for bonding and antibonding combinations. This result arises from placement of the oxygen molecule on the negative z axis.

globin and myoglobin.[30] For the sake of simplicity, therefore, we only consider here a linear configuration with the Fe-C-O axis perpendicular to the porphin plane. Table VI gives the atomic coordinates used. In contrast to the oxygen complex, the molecular orbital which derives from the degenerate π^* molecular orbital of the free carbon monoxide molecule is 3 eV above the top-filled molecular orbital.

To estimate transition frequencies for the carbon monoxide complex we followed the procedure of Zerner et al.[4] For charge-transfer transitions that originate or terminate in porphin π or π^* orbitals, electron exchange between the porphin and either metal or axial ligand is neglected. The transition energy, then, is simply the difference between the energies of the donor and acceptor orbitals. For iron d → d transitions we added an exchange energy to the orbital energy difference, which was calculated from crystal field theory. THE Racah parameters were obtained for this calculation by interpolating between the values for neutral and singly charged iron, using the calculated net charge on the iron of +0.2. An exchange energy correction of 0.5 eV was used for the iron(d) → CO(π^*) transition.[4]

Figure 6 shows the calculated transition frequencies for the carbon monoxide complex. We have classified the transitions into four types: iron d → d, iron(d) → porphin(π^*), porphin(π) → iron(d), and promotions into the CO(π^*) orbital from either an iron d orbital or porphin(π) orbital. The electric dipole transition moment direction is indicated next to each energy level. Magnetic-dipole polarizations are also indicated for the d → d transitions. The carbon monoxide model complex has strictly only C_s symmetry, but the retention of the degeneracies in the calculated orbital energies suggested that we use selection rules derived from a point group with a fourfold rotation axis. The polarization directions in Figure 6, therefore, are for C_{4v} symmetry. Figure 6 also shows the observed frequencies for bands I and II found in the CD spectrum of carbonmonoxyhemoglobin.

Figure 7 shows the observed and predicted frequencies for oxyhemoglobin with selection rules from C_s symmetry. Anticipating a possible assignment for band VII, the predicted frequency for the electronic promotion from the descendent of the x component of the degenerate π_u molecular orbital of the free oxygen molecule into the lowest empty molecular orbital is also included in Figure 7. As with the carbon monoxide complex, electron exchange for promotions into or out of porphin π or π^* orbitals was neglected. For all other transitions a single value of 0.5 eV was added to the orbital energy difference. Such an approximation should introduce an error in the predicted transition frequencies which is much smaller than other errors inherent in the extended Hückel method.[31]

Since the lowest empty molecular orbital is only 0.24 eV above the top-filled molecular orbital (Figure 5), use of a 0.5-eV exchange energy implies a triplet ground state. It has been known for some time, however, that the ground state of oxyhemoglobin is diamagnetic.[32] We have therefore only considered transitions originating from the singlet configuration in Figure 5. Cerdonio et al. have recently reported the presence of a low-lying paramagnetic state in oxyhemoglobin from magnetic susceptibility measurements in the range 25-250 K.[33] They analyzed their results in terms of a triplet state 146 cm^{-1} above the ground singlet. The interpretation of Cerdonio et al. has been questioned by Pauling, who attributes the paramagnetism in their frozen samples to partial dissociation of oxygen, and argues that oxyhemoglobin is completely diamagnetic at room temperature.[34]

D. Theoretical Estimates of Deoxyhemoglobin Transition Frequencies. As a model chromophore for deoxyhemoglobin we used a neutral, five-coordinate complex of iron-porphin and imidazole. Extended Hückel calculations were carried out on several geometries, with both domed and planar rings, and with the iron displaced between 0.42 and 0.62 Å from the plane of the four pyrrole nitrogens. Although the resulting molecular orbital energies reflected the changes in geometry, the basic orbital pattern was unchanged by these variations. Figure 5 shows the orbital energy levels obtained from a calculation using the atomic coordinates in Table VI, in which the porphin was taken to be planar, and the iron was displaced 0.62 Å from the porphin plane. Doming of the porphin ring, with the iron displaced 0.62 Å from the plane of the pyrrole nitrogens, changed these orbital energies by less than 0.05 eV.

Since the iron in deoxyhemoglobin is known from magnetic susceptibility and Mössbauer studies to be in a d^6 high-spin ground state,[35] the calculations were constrained by assigning one electron to each of the four highest d orbitals. In all geometries the $d_{x^2-y^2}$ orbital was found to be lowest in energy, and therefore contained the sixth d electron. Assignment of the sixth d electron to the correct orbital, i.e., knowing the correct ground state d electron configuration, is of course essential for the interpretation of the optical spectrum. To obtain the correct ground state configuration we appealed to the results of Eicher and co-workers. From a crystal field theoretical analysis of deoxyhemoglobin Mössbauer and magnetic susceptibility data, Eicher et al. and Huynh et al. concluded that there is a significant rhombic distortion of the heme complex, and that the ground state consists mainly of a configuration in which the d_{xz} orbital is doubly occupied.[36] The crystal field results should be much more reliable than the extended Hückel calculations in ordering the d orbitals. In calculating transition frequencies, therefore, we have assumed that d_{xz} is doubly occupied and that the energies of the d_{xz}, d_{yz}, and $d_{x^2-y^2}$ orbitals are all the same. This latter assumption is justified by

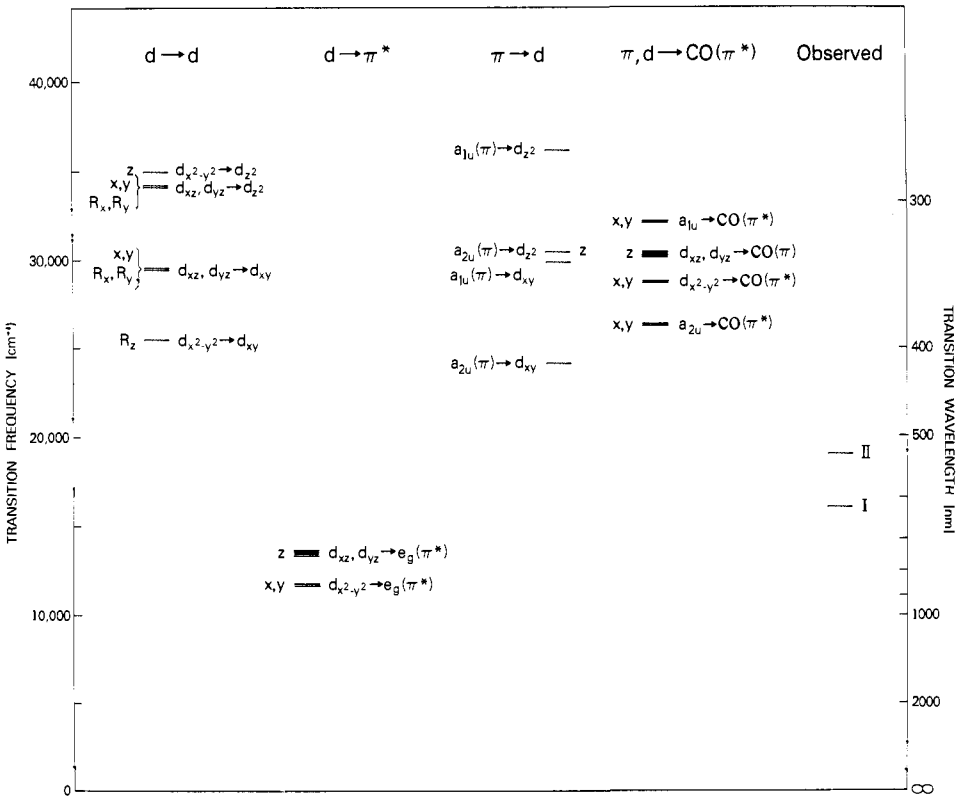

Figure 6. Predicted transition frequencies for the complex of iron-porphin with imidazole and carbon monoxide, and observed frequencies for carbonmonoxyhemoglobin. Electric-dipole selection rules are those of C_{4v} symmetry. Magnetic-dipole selection rules are also indicated for the d → d transitions. The frequencies are calculated using the orbital energy differences from Figure 5. No correction for electron exchange was made for the iron(d) → porphin(π^*), porphin(π) → iron(d), or porphin(π) → CO(π^*) transitions. An exchange energy of 4030 cm^{-1} (0.5 eV) was added to the orbital energy difference for the iron(d) → CO(π^*) transitions.[4] For the d → d transitions the following exchange energies were added to the orbital energy differences: $4B + C = 6100$ cm^{-1} for $d_{x^2-y^2} \rightarrow d_{z^2}$, $C = 2900$ cm^{-1} for $d_{x^2-y^2} \rightarrow d_{xy}$, $B + C = 3700$ cm^{-1} for d_{xz}, $d_{yz} \rightarrow d_{z^2}$, and $3B + C = 5300$ cm^{-1} for d_{xz}, $d_{yz} \rightarrow d_{xy}$. See footnote to Table VIII.

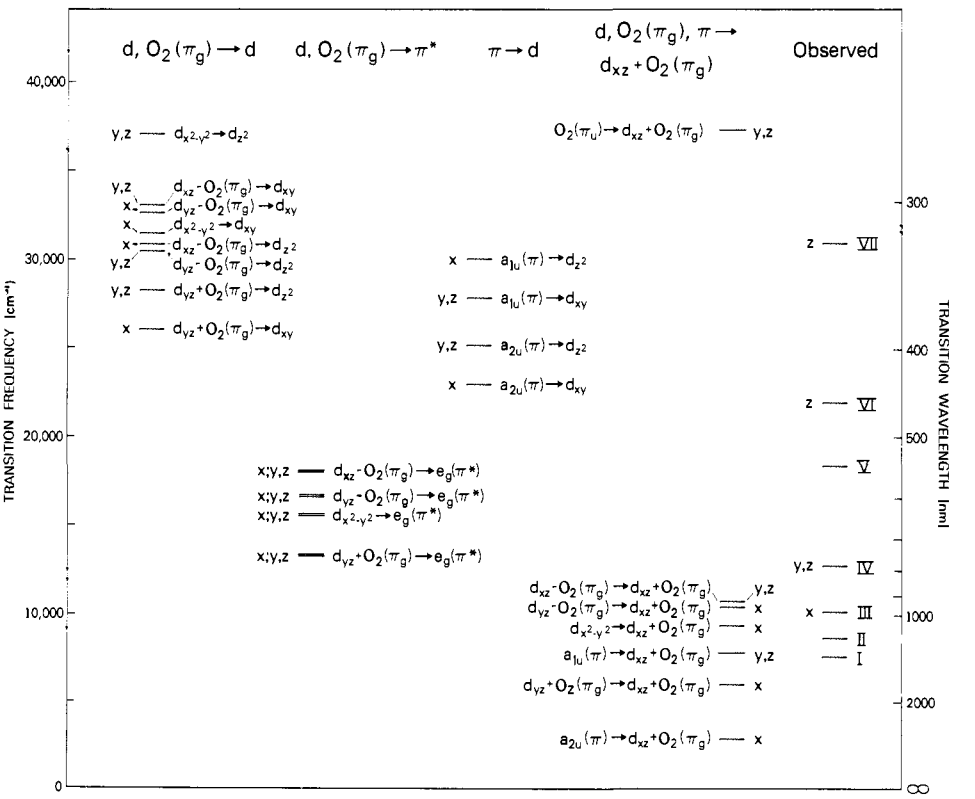

Figure 7. Predicted frequencies for the complex of iron-porphin with imidazole and oxygen, and observed frequencies for oxyhemoglobin. Electric-dipole selection rules are those of C_s symmetry. The frequencies are calculated using the orbital energy differences from Figure 5. No correction for electron exchange was made for transitions originating or terminating in porphin π orbitals. For all other transitions 4030 cm^{-1} (0.5 eV) was added to the orbital energy difference.

Table VII. Calculation of Exchange Energies for Selected Terms

configuration[a]	average term[b] energy	individual term energy	Δ[c]
$d^5\ e^2b_2a_1b_1$	$-20B + 6C$[d]	$^6A_1$: $-35B$	$-15B - 6C$
		$^4B_1$: $-22B + 5C$	$-2B - C$
$e^3b_2a_t$	$-13\frac{2}{3}B + 8C$	^4E: $-19B + 6C$	$-5\frac{1}{3}B - 2C$
$e^3b_2a_1$	$-13\frac{2}{3}B + 8C$	^4E: $-19B + 6C$	$-5\frac{1}{3}B - 2C$
$e^2b_2a_1b_1$	$-13\frac{2}{3}B + 8C$[d]	$^4A_2$,$^4B_2$: $-19B + 6C$	$-5\frac{1}{3}B - 2C$
$e^3b_2b_t$	$-19B + 8C$	^4E: $-23B + 6C$	$-4B - 2C$
$d^6\ e^3b_2a_1b$	$-11B + 4C$	^5E: $-21B$	$-10B - 4C$
$e^2b_2^2a_1b_t$	$-11B + 4C$[d]	$^5B_2$: $-21B$	$-10B - 4C$
$e^2b_2a_1^2b_1$	$-11B + 4C$[d]	$^5A_1$: $-21B$	$-10B - 4C$
$e^2b_2a_1b_1^2$	$-11B + 4C$[d]	$^5B_1$: $-21B$	$-10B - 4C$
$d^7\ e^4b_2a_1b_1$	$-6\frac{2}{3}B + 2C$	$^4A_2$: $-12B$	$-5\frac{1}{3}B - 2C$
$e^3b_2^2a_1b_1$	$-6\frac{2}{3}B + 2C$	^4E: $-12B$	$-5\frac{1}{3}B - 2C$
$e^3b_2a_1b_1^2$	$-6\frac{2}{3}B + 2C$	^4E: $-12B$	$-5\frac{1}{3}B - 2C$
$e^3b_2a_1^2b_1$	$-2B + 2C$	^4E: $-6B$	$-4B - 2C$

[a] The orbital labels are those of C_{4v} symmetry: e = $d_{xz}d_{yz}$; $b_1 = d_{x^2-y^2}$; $a_1 = d_{z^2}$; $b_2 = d_{xy}$. [b] This is the average of the electrostatic energies for all terms of a given configuration, taken from the tables of Ōtsuka.[38] B and C are Racah parameters. [c] Δ is the individual term energy minus the average term energy. [d] Only configurations in which the two electrons are in different e orbitals are included in this term average.

Table VIII. Exchange Correction to Orbital Energy Difference Used in Calculating Deoxyheme Transition Frequencies

orbital promotion	exchange correction[a] Racah parameters	cm^{-1}
$d_{xz} \rightarrow d_{x^2-y^2}, d_{xz}, d_{z^2}, d_{xy}$	0	0
$d_{xz} \rightarrow$ porphin(π^*)	$-5B - 2C$	−9800
	$8B + 3C$	15 100
$d_{yz} \rightarrow$ porphin(π^*)	$4\frac{2}{3}B + 2C$	9500
$d_{x^2-y^2} \rightarrow$ porphin(π^*)	$4\frac{2}{3}B + 2C$	9500
$d_{z^2} \rightarrow$ porphin(π^*)	$6B + 2C$	10 600
$d_{xy} \rightarrow$ porphin(π^*)	$4\frac{2}{3}B + 2C$	9500
porphin(π) $\rightarrow d_{yz}$	$4\frac{2}{3}B + 2C$	9500
porphin(π) $\rightarrow d_{x^2-y^2}$	$4\frac{2}{3}B + 2C$	9500
porphin(π) $\rightarrow d_{z^2}$	$6B + 2C$	10 600
porphin(π) $\rightarrow d_{xy}$	$4\frac{2}{3}B + 2C$	9500

[a] These are calculated from the differences in the Δ values given in Table VI. The energies in cm^{-1} were calculated using B = 800 cm^{-1} and C = 2900 cm^{-1}, which are very close to the values obtained by interpolating between the Fe^0 and Fe^+ Racah parameters (B = 806, 782; C = 2660, 3955 cm^{-1}), using the extended Hückel calculated net charge on the iron of +0.18.

the calculation of Eicher et al. that the d_{xz}-$d_{x^2-y^2}$ and d_{xz}-d_{yz} separations are only 380 and 760 cm^{-1}, respectively.[36a,50]

The procedure for estimating exchange energy corrections in calculating transition frequencies is more complicated for deoxyheme than for the oxygen or carbon monoxide complexes. Many more terms of differing spin multiplicity derive from a single electron configuration. Following Zerner et al. the exchange energy for a particular term of a given electron configuration was taken as the difference between the exchange energy for that term and the average of the exchange energies for all of the terms which derive from that configuration.[4] Only a few of the relevant energy expressions were given by Zerner et al. and Zerner.[4,37] The work of Ōtsuka, however, contains all of the necessary energies.[38] Ōtsuka calculated the first-order electrostatic energy for every term that derives from a given electron configuration for all d^5, d^6, and d^7 configurations in C_{4v} symmetry. These energies contain both the Coulomb repulsion and electron exchange contributions. The Coulomb repulsion contribution to the term energy is, however, the same for all terms that derive from the same configuration. Therefore the difference between an individual term energy and the average term energy is a pure exchange energy, which we call Δ. Table VII shows the calculation of Δ in terms of Racah parameters for all of the terms that arise in considering deoxyheme transitions. The difference between Δ for an excited configuration and Δ for the ground state configuration is the exchange energy that must be added to the orbital energy difference to obtain a transition frequency.[4] These exchange corrections for the various spin-allowed d → d and charge-transfer promotions are given in Table VIII. As before, iron-porphin electron exchange has been neglected.

Figure 8 shows the observed and calculated transition frequencies for deoxyheme, using the orbital energy differences from Figure 5 and the exchange energy corrections from Table VIII. Since no axial ligand orbitals appear in the energy region of the top-filled and lowest empty molecular orbitals, only three classes of transitions must be considered: iron d → d, iron(d) → porphin(π^*), and porphin(π) → iron(d). The polarizations are those of C_{2v} symmetry, the point group used by Eicher et al. in their crystal field analysis of deoxyhemoglobin.[36] Figure 8 also shows the predicted frequencies of the d → d transitions obtained from the crystal field parameters of Eicher et al.[36,50]

Discussion

A. Assignment of Carbonmonoxyhemoglobin Transitions. Before discussing the assignments for oxyhemoglobin it is useful to consider the spectrum of the carbon monoxide complex. The optical spectrum of carbonmonoxyhemoglobin is very much like that of a closed-shell metal porphyrin,[6a] which generally only exhibits porphyrin $\pi \rightarrow \pi^*$ Q, B, and N bands below 33 000 cm^{-1}.[39] Makinen and Eaton could find no evidence for additional bands in either the crystal or solution absorption spectra.[6a] A particularly important negative finding was the lack of any near-infrared electronic absorption.[6a] A recent near-ultraviolet-visible MCD study of carbonmonoxymyoglobin by Vickery et al.[40] also provides no obvious evidence for additional transitions. Thus far only the CD spectrum has been informative in this regard. Two bands, labeled I and II, are observed in the CD spectrum of carbonmonoxyhemoglobin at 16 000 and 17 850 cm^{-1}, which cannot be associated with the porphyrin Q bands that dominate the absorption in this region (Figure 2 and Table II). Eaton and Charney reported CD bands at similar frequencies for carbonmonoxymyoglobin.[7b,c] In the 4000-33 000 cm^{-1} frequency range, then, only two transitions have been observed for the carbon monoxide complex which are not porphyrin $\pi \rightarrow \pi^*$.

In contrast to the experimental finding of only two transitions, Figure 6 shows that a large number of charge-transfer

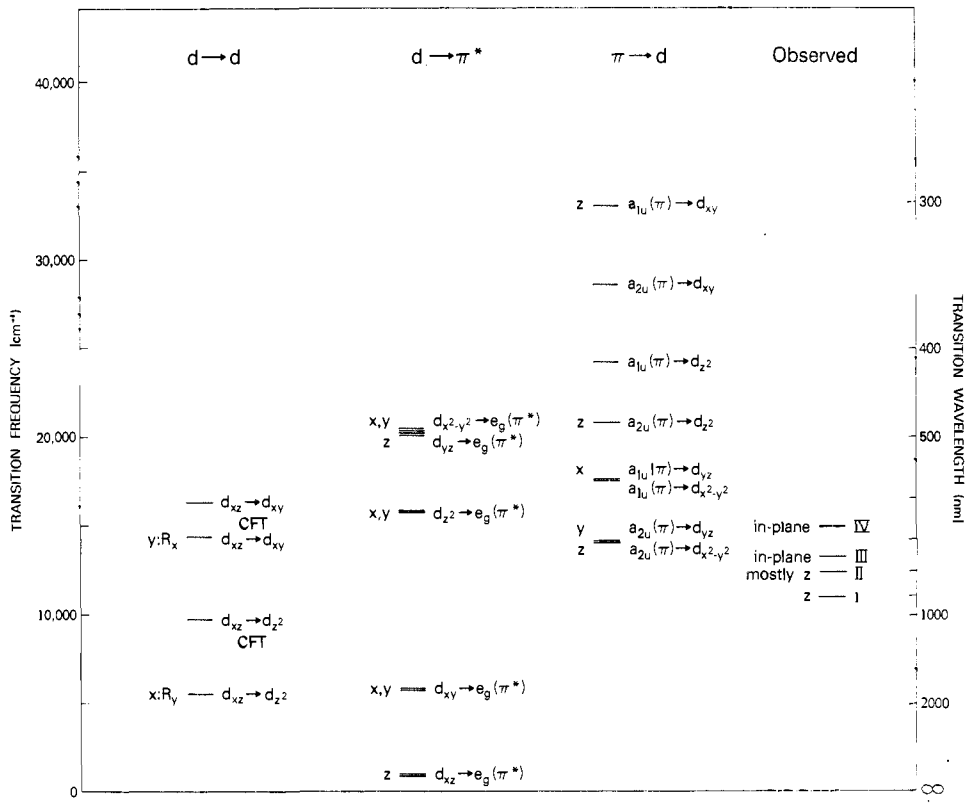

Figure 8. Predicted frequencies for the complex of iron-porphin with imidazole and observed frequencies for deoxyhemoglobin. Electric and magnetic-dipole selection rules are those of C_{2v} symmetry. The frequencies are calculated using the orbital energy differences from Figure 5, except that the energies of the d_{xz}, d_{yz}, and $d_{x^2-y^2}$ orbitals are assumed to be the same. The crystal field analysis of Eicher et al. predicts the $d_{xz} \rightarrow d_{x^2-y^2}$ and $d_{xz} \rightarrow d_{yz}$ transitions to appear at 380 and 760 cm^{-1}, respectively.[36a] See text and Table VIII for exchange energy corrections. CFT refers to the crystal field theoretical frequency predicted by Eicher et al.[36a]

and d → d transitions are predicted from our extended Hückel calculations to appear in the experimentally accessible frequency range. Iron(d) → porphin(π^*) charge-transfer transitions are closest to the observed frequencies, and are therefore obvious candidates. The single crystal data, however, argue against such an interpretation, since there is no evidence for any z-polarized intensity as would be expected for the d_{xz}, d_{yz} → $e_g(\pi^*)$ transitions. The most plausible assignment for bands I and II, then, is that they correspond to iron d → d transitions, as originally suggested by Eaton and Charney on the basis of their relatively large CD anisotropy factors.[7b,c]

The diamagnetism and small Mössbauer quadrupole splitting characterize the iron in carbonmonoxyhemoglobin as a d^6 low-spin ion.[32-34,35a] In tetragonal symmetry, such as C_{4v}, the two lowest d → d transitions are the magnetic-dipole allowed $^1A_1 \rightarrow {}^1A_2$ ($d_{x^2-y^2} \rightarrow d_{xy}$) and $^1A_1 \rightarrow {}^1E$ (d_{xz}, $d_{yz} \rightarrow d_{z^2}$, d_{xy}). Although these transitions are expected to give rise to weak absorption bands because of the forbidden electric-dipole character of d → d transitions, the large magnetic dipole transition moments can potentially make the $^1A_1 \rightarrow {}^1A_2$, ^1E transitions prominent in the CD spectrum. Eaton and Charney used the criteria of weak absorption and large CD anisotropy factor to locate these transitions in the 12 000-16 000-cm^{-1} region of ferrocytochrome c, in which the axial ligands are histidyl and methionyl residues.[7b,c] Since carbon monoxide is expected to have a larger ligand field strength than methionine, these d → d transitions are predicted to be at higher frequencies in carbonmonoxyhemoglobin, in agreement with the above assignment. The magnetic polarizations of $^1A_1 \rightarrow {}^1A_2$ and $^1A_1 \rightarrow {}^1E$ are z and x,y, respectively. $^1A_1 \rightarrow {}^1A_2$ therefore requires z-polarized electric-dipole intensity to produce CD, while $^1A_1 \rightarrow {}^1E$ requires x,y-polarized electric-dipole intensity. Since only x,y-polarized electric-dipole intensity is observed in the crystal spectrum, we assign the weaker band I to $^1A_1 \rightarrow {}^1A_2$ and $^1A_1 \rightarrow {}^1E$ to the more intense, broader band II.

Although the absolute frequency predictions of the extended Hückel calculations for these d → d transitions in Figure 6 appear to be in error by nearly 10 000 cm^{-1}, the theoretical results do predict the correct ordering of the $^1A_2$ and ^1E states. The failure to observe the iron(d) → porphin(π^*) transitions using any of the polarized light techniques indicates that they lie above the very intense Soret (B) band at about 24 000 cm^{-1}, suggesting that the extended Hückel calculations are underestimating these transitions by at least 10 000 cm^{-1}. Furthermore, the absence of the porphin(π) → iron(d) and iron(d), porphin(π) → CO(π^*) charge-transfer bands suggests that the predicted frequencies represent minimum values for these transitions.

B. Assignment of Oxyhemoglobin Transitions. Thus far we have found seven transitions in the optical spectra of oxyhemoglobin in addition to the porphyrin $\pi \rightarrow \pi^*$ transitions. The experimental results for bands I-VI are given in Figures 1 and 2 and in Tables I and II. Band VII appears in the crystal spectrum measured by Makinen and Eaton as a z-polarized transition at about 31 000 cm^{-1} (ϵ 4400 M^{-1} cm^{-1}, $f = 0.15$, $\nu_{1/2} = 4600$ cm^{-1}).[6a] With these experimental results and the MCD data of others for the visible and near-ultraviolet spectral regions, we attempt to assign all seven transitions using the extended Hückel results in Figure 7.

The most unambiguous assignments can be made for the near-infrared bands I-IV, since Figure 7 indicates that the number of possible transitions decreases with decreasing frequency. We assign bands I-IV to transitions involving electronic promotions into the lowest empty molecular orbital (d_{xz} + $O_2(\pi_g)$), which is a mixture of iron d_{xz} and the x component of the free oxygen π_g molecular orbital. Six such transitions are predicted to appear below 11 000 cm^{-1}. Two of them (d_{yz} + $O_2(\pi_g)$, $d_{x^2-y^2} \rightarrow d_{xz}$ + $O_2(\pi_g)$) have substantial mag-

Table IX. Assignments of Oxyhemoglobin Transitions

band	frequency, cm^{-1}	oscillator strength	polarization	orbital promotion
I	7700	<0.000 05		$d_{yz} + O_2(\pi_g) \rightarrow d_{xz} + O_2(\pi_g)$
II	8700	<0.0003		$d_{x^2-y^2} \rightarrow d_{xz} + O_2(\pi_g)$
III	10 200	0.0026	x	$a_{2u}(\pi) \rightarrow d_{xz} + O_2(\pi_g)$
IV	12 800	0.0021	y,z	$a_{1u}(\pi) \rightarrow d_{xz} + O_2(\pi_g)$
Q_o,Q_v	17 900	0.12	x,y	$a_{1u}(\pi)$,$a_{2u}(\pi) \rightarrow e_g(\pi^*)$
V	18 400			$d \rightarrow d$
VI	22 000	0.022	z	$d \rightarrow d$
B	24 100	1.3	x,y	$a_{1u}(\pi)$,$a_{2u}(\pi) \rightarrow e_g(\pi^*)$
N	29 000	0.54	x,y	$a_{2u}(\pi)$,$b_{2u}(\pi) \rightarrow e_g(\pi^*)$
VII	31 000	0.15	z	$O_2(\pi_u) \rightarrow d_{xz} + O_2(\pi_g)$

netic-dipole allowed iron d → d and oxygen p → p character, and would therefore be expected to produce weak absorption bands with large CD anisotropy factors. This is precisely what is observed for bands I and II (Table I). Assuming that the order of these transitions given by the extended Hückel calculations is correct, we can assign bands I and II to the $d_{yz} + O_2(\pi_g) \rightarrow d_{xz} + O_2(\pi_g)$ and $d_{x^2-y^2} \rightarrow d_{xz} + O_2(\pi_g)$ electronic promotions, respectively.

Assignment of bands III and IV to the $a_{2u}(\pi) \rightarrow d_{xz} + O_2(\pi_g)$ and $a_{1u}(\pi) \rightarrow d_{xz} + O_2(\pi_g)$ charge-transfer transitions is consistent with all of the results in Table I. The oscillator strengths for these bands are comparable to the values for the $a_{1u}(\pi)$, $a_{2u}(\pi) \rightarrow d_{xz}$, d_{yz} charge-transfer transitions that appear in the near-infrared spectra of high- and low-spin ferric heme proteins.[6b,6c] Neither charge-transfer transition has any intrinsic magnetic-dipole strength, in agreement with the low observed CD anisotropy factor. The assignments are also consistent with the observed variation in the polarization ratio (Figure 1c). Since band IV is predicted to have a z-polarized component, it should exhibit a lower polarization ratio than band III, as is observed (Gaussian resolution of the crystal spectra results in polarization ratios of 2.4 and 2.0 for bands III and IV). Finally, the assignments are in good agreement with the observed MCD. Assuming that bands III and IV are polarized wholly along x and y, respectively, the B terms produced by the interaction of the two excited states are equal and of opposite sign with anisotropy factors:

$$g_{III} = 0.92 \left(\frac{f_{IV}}{f_{III}}\right)^{1/2} \frac{\mu}{\Delta E}$$

and

$$g_{IV} = 0.92 \left(\frac{f_{III}}{f_{IV}}\right)^{1/2} \frac{\mu}{\Delta E}$$

where μ is the magnitude in Bohr magnetons of the z component of the magnetic-dipole matrix element connecting the excited states of transitions III and IV, and ΔE is their separation in cm^{-1}.[41] μ can be further equated to the one-electron matrix element of the orbital angular momentum operator, $|\langle a_{2u}|l_z|a_{1u}\rangle|$. Substitution of the values for g_{III}, g_{IV}, f_{III}, f_{IV}, and ΔE from Table I then leads to $|\langle a_{2u}|l_z|a_{1u}\rangle| = 1.4$–$1.6$. It is well known from prior analyses of metalloporphyrin MCD that the orbital angular momentum of porphyrin orbitals can be very large. In particular, experimental and theoretical evaluations of $|\langle a_{2u}|l_z|a_{1u}\rangle|$ have yielded magnitudes in the range 1.5–4.5.[42] For oxyhemoglobin, the MCD data of Dratz[43] for the Q and B bands lead to a value of approximately 1.5. the excellent agreement between the values for $|\langle a_{2u}|l_z|a_{1u}\rangle|$ derived from the near-infrared and visible MCD data is strong confirmation of the assignment of bands III and IV. It should be emphasized further that the very large μ obtained is considerably greater than the upper limit we would expect for any alternative assignments for bands III and IV, not involving porphyrin orbitals.

Assignment of bands V, VI, and VII is more difficult. Figure 2 and Table II show that CD bands V and VI have similar characteristics to bands I and II observed in the CD spectrum of carbonmonoxyhemoglobin. Furthermore, the MCD spectra in the region of bands V and VI show no additional transitions.[40,51] It is reasonable, then, to assign bands V and VI to d → d transitions analogous to bands I and II of the carbon monoxide complex. Since these d → d transitions have no intrinsic electric-dipole intensity, the substantial z-polarized intensity of band VI would have to be ascribed to vibrational borrowing from the much more intense z-polarized band VII. The extended Hückel calculations are consistent with this assignment in that the mainly d → d transitions shown in the first column of Figure 7 are predicted to appear in the same frequency range as those predicted for the carbon monoxide complex (see Figure 6). We do not believe, however, that the extended Hückel frequencies are sufficiently accurate to make more detailed assignments. Conventional ligand field theory, moreover, is not applicable because of the strong mixing of the iron d and oxygen π_g orbitals.

The final transition to assign is band VII. The large z-polarized intensity of band VII ($f = 0.15$) indicates that this transition is strongly electric-dipole allowed. The valence bond calculations of Goddard and Olafson on the triatomic molecule FeO_2 suggest a possible assignment.[44] They proposed that band VII is the analogue of the Hartley ozone band, in which electron density is transferred from the central oxygen atom to the outer atoms. A similar transition, $O_2(\pi_u) \rightarrow d_{xz} + O_2(\pi_g)$, is predicted by the extended Hückel calculations to appear at 37 000 cm^{-1}, close to the observed frequency of 31 000 cm^{-1} for band VII. The dominant contribution to the $O_2(\pi_u)$ molecular orbital is the p_x atomic orbital on the proximal oxygen atom, while the $d_{xz} + O_2(\pi_g)$ molecular orbital contains nearly equal contributions from the iron d_{xz}, and the p_x atomic orbitals on the proximal and distal oxygens. Thus the $O_2(\pi_u) \rightarrow d_{xz} + O_2(\pi_g)$ excitation would result in the same transfer of electron density as is found in the valence bond calculations.[44]

Our assignments for oxyhemoglobin are summarized in Table IX. We regard the assignments of bands I–IV to transitions into the lowest empty molecular orbital as considerably more certain than our assignments of bands V–VII. The extended Hückel frequencies in Figure 7 suggest that many alternative assignments for the latter bands are plausible, and we do not believe that the present experimental and theoretical information is sufficient to distinguish clearly among them. For example, bands V and VI in the CD spectrum could arise from d → d transitions, while the z-polarized band VI in the absorption spectrum could correspond to a separate electronic transition. Candidates are the $d_{xz} - O_2(\pi_g) \rightarrow d_{xz} + O_2(\pi_g)$, imidazole ($\pi$) → $d_{xz} + O_2(\pi_g)$, or the $a_{2u}(\pi) \rightarrow d_{z^2}$ charge-transfer transitions, since of the numerous possibilities these might be expected to have observable z-polarized electric-dipole intensity. The absence of iron(d) → porphin(π^*) tran-

Table X. Assignments of Deoxyhemoglobin Transitions

band	frequency, cm^{-1}	oscillator strength	polarization	orbital promotion
I	10 900	0.000 91	z	$d_{xz} \rightarrow e_g(\pi^*)$
II	12 300	0.001	mostly z	$d_{xz} \rightarrow d_{z^2}$
III	13 200	0.000 33	in-plane	$a_{2u}(\pi) \rightarrow d_{yz}$
IV	14 900	0.0002	in-plane	$a_{1u}(\pi) \rightarrow d_{yz}$
Q_0-Q_v	17 500	0.15	x,y	$a_{1u}(\pi),a_{2u}(\pi) \rightarrow e_g(\pi^*)$
B	23 250	1.2	x,y	$a_{1u}(\pi),a_{2u}(\pi) \rightarrow e_g(\pi^*)$

sitions in carbonmonoxyhemoglobin makes the assignment of the observed bands of oxyhemoglobin to transitions of this type less probable.

Alternative assignments for bands VI and VII have recently been proposed by Churg and Makinen on the basis of a comparative single crystal study of the oxygen and cyanide complexes of myoglobin, which they report exhibit z-polarized bands of similar frequency and intensity.[53] They therefore assumed that neither band VI nor VII could involve oxygen orbitals, and proposed that both bands arise from porphin(π) $\rightarrow$ iron(d) charge-transfer transitions. Band VI was assigned to the $a_{1u}(\pi) \rightarrow d_{z^2}$ transition with the z-polarized intensity arising from vibronic coupling, presumably to band VII. Band VII was assigned to a cluster of promotions from the next highest filled pair of porphyrin orbitals, which include the $a_{2u}(\pi)$, $b_{2u}(\pi) \rightarrow d_{z^2}$ and $a_{2u}'(\pi)$, $b_{2u}(\pi) \rightarrow d_{xy}$ excitations.

C. Assignment of Deoxyhemoglobin Transitions. We have been able to describe four transitions in deoxyhemoglobin in addition to the porphyrin $\pi \rightarrow \pi^*$ transitions. All four bands appear in the near-infrared spectral region (Figure 3). The experimental parameters for these bands are summarized in Tables III and IV. At higher frequencies the absorption is dominated by the intense porphyrin Q and B bands. Although additional underlying transitions are most probably responsible for the diffuseness and complex shape of the Q and B bands, it is not possible to clearly delineate their contribution in any of the polarized light experiments.[49]

Use of the extended Hückel results for calculating transition frequencies is not as straightforward as with the carbon monoxide and oxygen complexes. The ground state of the iron in deoxyhemoglobin descends from an orbitally threefold degenerate $^5T_2$ state in octahedral symmetry. According to the crystal field analysis of Eicher et al. and Huynh et al. tetragonal and rhombic crystal fields remove this degeneracy, resulting in three orbitally nondegenerate states that are mixed by spin-orbit coupling.[36] About 75% of the ground state wave function is composed of the configuration, $d_{xz}^2\, d_{x^2-y^2} d_{yz} d_{z^2} d_{xy}$.[45] The extended Hückel calculations predict a different ground state configuration, $d_{x^2-y^2}^2 d_{xz} d_{yz} d_{z^2} d_{xy}$, with the $d_{x^2-y^2}$ orbital lowest in energy (Figure 5). The crystal field analysis should be more reliable, and we have therefore assumed that d_{xz} is lowest and doubly occupied in using the extended Hückel orbital energies to predict transition frequencies. This assumption has a major effect on the predicted frequencies and ordering of the excited states because of very large differences in the exchange corrections to the orbital energy differences (Table VIII). For example, if $d_{x^2-y^2}$ were doubly occupied, the lowest frequency transition would be the x,y-polarized $d_{x^2-y^2} \rightarrow e_g(\pi^*)$ charge-transfer transition instead of the z-polarized $d_{xz} \rightarrow e_g(\pi^*)$ transition predicted in Figure 8 with d_{xz} doubly occupied.

The most unambiguous assignment can be made for band I. It has two distinguishing characteristics. Band I is the lowest frequency transition, and it is almost purely z-polarized. The two lowest frequency z-polarized transitions are predicted to be the $d_{xz} \rightarrow e_g(\pi^*)$ and $a_{2u}(\pi) \rightarrow d_{x^2-y^2}$ charge-transfer transitions (Figure 8). Two factors argue in favor of $d_{xz} \rightarrow e_g(\pi^*)$ as the correct assignment. First, it is calculated to lie 13 000 cm^{-1} below the $a_{2u}(\pi) \rightarrow d_{x^2-y^2}$ transition. Second, it is electric-dipole allowed in both C_{2v} and C_{4v} symmetries (C_{2v} is the effective symmetry of the crystal field and the point group used in deriving the selection rules in Figure 8, while C_{4v} is the effective symmetry according to the extended Hückel calculations). Again we see that there is an apparent error of about 10 000 cm^{-1} in the extended Hückel frequency.

The CD, MCD, and crystal polarization data point to the assignment of bands III and IV as $a_{2u}(\pi) \rightarrow d_{yz}$ and $a_{1u}(\pi) \rightarrow d_{yz}$ charge-transfer transitions, respectively. The very low CD anisotropy factor for band III indicates that it is not a d $\rightarrow$ d transition, since both predicted d $\rightarrow$ d transitions are magnetic-dipole allowed.[46] The narrow widths of bands III and IV also argue against d $\rightarrow$ d assignments. No A terms appear in the MCD as might be expected for the effectively degenerate $d_{x^2-y^2}$, d_{xy}, $d_{z^2} \rightarrow e_g(\pi^*)$ charge-transfer transitions. Both bands are polarized more nearly parallel to the plane than perpendicular to it. Neither, however, is x,y polarized, also suggesting that they do not arise from degenerate transitions. The difference in polarization ratio for bands III and IV, moreover, indicates different directions in the heme plane for their electric-dipole transition moments, which is consistent with the predicted polarizations of y for $a_{2u}(\pi) \rightarrow d_{yz}$ and x for $a_{1u}(\pi) \rightarrow d_{yz}$.

The assignment of band II is somewhat more speculative because its spectroscopic parameters are so similar to those of band I. Band II has mixed polarization, but it is mostly z polarized, suggesting that it could be a vibronic component of the same electronic transition as band I. The separation between bands I and II is 1350-1850 cm^{-1} (Table III), however, which seems too large for a vibrational interval. Our assignment of band II is suggested by the crystal field analysis of Eicher et al.[36] Their d orbital splitting parameters predict the magnetic-dipole allowed $d_{xz} \rightarrow d_{z^2}$ and $d_{xz} \rightarrow d_{xy}$ transitions at 9800 and 16 200 cm^{-1}. Since crystal field theory is usually capable of predicting d $\rightarrow$ d transition frequencies to within a few thousand cm^{-1}, $d_{xz} \rightarrow d_{z^2}$ should be observable in the near-infrared CD spectrum, and is therefore the most likely candidate for band II. The lack of a large anisotropy factor is consistent with the orthogonality of the predicted magnetic (y) and the observed electric (mostly z) polarizations, but we do not have a good explanation for the predominantly z-polarized electric-dipole intensity of band II. Another possible assignment, therefore, is the $a_{2u} \rightarrow d_{x^2-y^2}$ transition.

Our assignments are summarized in Table X. In the above analysis we have used the MCD data mainly as further evidence that there are only four near-infrared bands. We have not yet carried out any measurements on the temperature dependence of the MCD spectra to delineate B and C term contributions. Such measurements are required before the MCD can be more helpful in making detailed assignments. Some data do exist for band III from the work of Nozawa et al. on deoxymyoglobin.[47] They found a small temperature dependence for this band, indicating that a B term is making the dominant contribution.

Conclusion

The experimental results presented here represent a major

extension of the information on the optical spectra of oxy- and deoxyhemoglobin. With the combined use of CD, MCD, and single crystal spectroscopies we have been able to characterize seven transitions of oxyhemoglobin and four transitions of deoxyhemoglobin, in addition to the porphyrin $\pi \rightarrow \pi^*$ transitions. From the experimental parameters and predictions of extended Hückel theory we have attempted to make detailed assignments for all of the observed transitions. Although by no means definitive, these assignments provide a useful basis for future experimental and theoretical investigations.

To further improve our understanding of these spectra it would seem worthwhile to carry out a similar experimental study on other heme proteins and model complexes. Such an investigation would permit the use of empirical comparisons to help interpret the spectra. It would be important to use as many optical methods as possible, since the present investigation demonstrates that a single technique is insufficient. Measurements at low temperatures, moreover, should aid in more clearly resolving the individual components of these overlapping, broad-banded spectra. Resonance Raman spectroscopy with near-infrared tunable lasers should also provide valuable new information.

Because of the large inaccuracies found in many of the predicted extended Hückel frequencies, calculations using more reliable quantum mechanical methods are clearly needed. In addition to transition frequencies, calculations of intensities, polarizations, and MCD amplitudes are important to distinguish among alternate assignments. If it becomes possible to describe the chirality of the heme complex and its environment, CD calculations for the near-infrared transitions might also be feasible.

Case, Huynh, and Karplus have recently carried out an extensive theoretical investigation of the ground and excited states of oxyhemoglobin using the extended Pariser-Parr-Pople and $X\alpha$ multiple scattering methods.[48,52] Their results, which include estimates of intensities and polarizations, are in accord with most of our assignments, although alternate possibilities are suggested in some cases. An $X\alpha$ calculation of deoxyhemoglobin is currently being completed by Case and Karplus.

Acknowledgment. We are indebted to Martin Gouterman and Sheldon Aronowitz for providing us with their extended Hückel computer program and for valuable advice in carrying out the calculations. We would like to thank Martin Karplus and David A. Case for several stimulating discussions and for the preprint of their theoretical study on oxyhemoglobin. We also thank Heisaburo Shindo for preparing human deoxyhemoglobin A crystals, H. Eicher for communicating unpublished results of his crystal field analysis of deoxyhemoglobin, Marvin W. Makinen for communicating results of his spectroscopic investigation of oxymyoglobin prior to publication, and Donna Becker for technical assistance. W.A.E. would like to acknowledge the collaboration of Marvin W. Makinen on some of the experimental work in the initial stages of this study. Work carried out at the University of Southern California was supported by the National Institutes of Health and the National Science Foundation.

References and Notes

(1) Author to whom reprint requests should be sent.
(2) (a) National Institutes of Health; (b) University of Southern California.
(3) (a) M. F. Perutz, J. E. Ladner, S. R. Simon, and C. Ho., *Biochemistry*, **13**, 2163–2173 (1974); (b) M. F. Perutz, A. R. Fersht, S. R. Simon, and G. C. K. Roberts, *ibid.*, **13**, 2174–2186 (1974); (c) M. F. Perutz, E. J. Heidner, J. E. Ladner, J. G. Beetlestone, C. Ho, and E. F. Slade, *ibid.*, **13**, 2187–2200 (1974); (d) B. I. Greene, R. M. Hochstrasser, R. B. Weisman, and W. A. Eaton, *Proc. Natl. Acad. Sci., U.S.A.*, in press.
(4) M. Zerner, M. Gouterman, and H. Kobayashi, *Theor. Chim. Acta*, **6**, 363–400 (1966).
(5) W. A. Eaton and R. M. Hochstrasser, *J. Chem. Phys.*, **49**, 985–995 (1968).
(6) (a) M. W. Makinen and W. A. Eaton, *Ann. N.Y. Acad. Sci.*, **206**, 210–222 (1973); (b) J. C. Cheng, G. A. Osborne, P. J. Stephens, and W. A. Eaton, *Nature (London)*, **241**, 193–194 (1973); (c) P. J. Stephens, J. C. Sutherland, J. C. Cheng, and W. A. Eaton, "The Excited States of Biological Molecules", J. B. Birks, Ed., Wiley, New York, N.Y., 1976, pp 434–442.
(7) (a) W. A. Eaton and R. M. Hochstrasser, *J. Chem. Phys.*, **46**, 2533–2539 (1967); (b) W. A. Eaton and E. Charney, *ibid.*, **51**, 4502–4505 (1969); (c) W. A. Eaton and E. Charney, "Probes of Structure and Function of Macromolecules and Membranes," Vol. I, B. Chance, C. P. Lee, and J. K. Blasie, Ed., Academic Press, New York, N.Y., 1971, pp 155–164; (d) J. C. Sutherland, D. Axelrod, and M. P. Klein, *J. Chem. Phys.*, **54**, 2888–2898 (1971).
(8) J. Rawlings, P. J. Stephens, L. A. Nafie, and M. D. Kamen, *Biochemistry*, **16**, 1725–1729 (1977).
(9) (a) L. K. Hanson, W. A. Eaton, S. G. Sligar, I. C. Gunsalus, M. Gouterman, and C. R. Connell, *J. Am. Chem. Soc.*, **98**, 2672–2674 (1976); (b) L. K. Hanson, S. G. Sligar, and I. C. Gunsalus, *Croat. Chim. Acta*, **49**, 237–250 (1977).
(10) W. A. Eaton, J. Hofrichter, L. K. Hanson, and M. W. Makinen, "Metalloprotein Studies Utilizing Paramagnetic Effect of the Metal Ions as Probes", M. Kotani and A. Tasaki, Ed., Osaka University, Osaka, Japan, 1975, pp 51–85.
(11) M. F. Perutz, *J. Cryst. Growth*, **2**, 54–56 (1968).
(12) (a) W. A. Eaton and T. P. Lewis, *J. Chem. Phys.*, **53**, 2164–2172 (1970); (b) W. A. Eaton, J. Hofrichter, M. W. Makinen, R. D. Andersen, and M. L. Ludwig, *Biochemistry*, **14**, 2146–2151 (1975).
(13) M. F. Perutz, I. F. Trotter, E. R. Howells, and D. R. Green, *Acta Crystallogr.*, **8**, 241–245 (1955).
(14) J. Hofrichter, D. G. Hendricker, and W. A. Eaton, *Proc. Natl. Acad. Sci. U.S.A.*, **70**, 3604–3608 (1973).
(15) (a) G. A. Osborne, J. C. Cheng, and P. J. Stephens, *Rev. Sci. Instrum.*, **44**, 10–15 (1973); (b) L. A. Nafie, T. A. Keiderling, and P. J. Stephens, *J. Am. Chem. Soc.*, **98**, 2715–2723 (1976).
(16) J. C. Sutherland, P. J. Stephens, W. A. Eaton, and B. M. Sutherland, Abstracts of Pacific Conference on Chemistry and Spectroscopy, San Diego, Calif., Nov 1973.
(17) J. C. Sutherland, L. E. Vickery, and M. P. Klein, *Rev. Sci. Instrum.*, **45**, 1089–1094 (1974).
(18) G. D. Knott and D. K. Reece, "Proceedings of the ONLINE '72 International Conference", Vol. 1, Brunel University, England, 1972, pp 497–526; (b) G. D. Knott and R. I. Shrager, "Proceedings of the SIGGRAPH Computers in Medicine Symposium," Vol. 6, No. 4, ACM, SIGGRAPH Notice, 1972, pp 138–151.
(19) (a) T-K. Li and B. P. Johnson, *Biochemistry*, **8**, 3638–3643 (1969); (b) Y. Ueda, T. Shiga, and I. Tyuma, *Biochem. Biophys. Res. Commun.*, **35**, 1–5 (1969); (c) H. Hamaguchi, A. Isomoto, and H. Nakajima, *ibid.*, **35**, 6–11 (1969); (d) Y. Ueda, T. Shiga, and I. Tyuma, *Biochim. Biophys. Acta*, **207**, 18–29 (1970); (e) M. W. Makinen and H. Kon, *Biochemistry*, **10**, 43–52 (1971).
(20) Another possible interpretation of the negative CD in Figure 2a is that it arises from two negative CD bands at 17 050 and 19 100 cm^{-1}. In this case the 17 050-cm^{-1} band would be regarded as one of the components of the Q_0 band, and the 19 100-cm^{-1} band as band V.
(21) (a) M. W. Makinen and W. A. Eaton, unpublished results; (b) *Nature (London)*, **247**, 62–64 (1974).
(22) H. C. Watson and C. L. Nobbs, "Biochemie des Sauerstoffs", B. Hess and H. J. Staudinger, Ed., Springer-Verlag, West Berlin, 1968, pp 37–48.
(23) L. Pauling, "Haemoglobin", F. J. W. Roughton and J. C. Kendrew, Ed., Butterworths, London, 1949, pp 57–65.
(24) (a) J. P. Collman, R. R. Gagne, C. A. Reed, W. T. Robinson, and G. A. Rodley, *Proc. Natl. Acad. Sci. U.S.A.*, **71**, 1326–1329 (1974); (b) J. P. Collman, R. R. Gagne, C. A. Reed, T. R. Halbert, G. Lang, and W. T. Robinson, *J. Am. Chem. Soc.*, **97**, 1427–1439 (1975).
(25) J. P. Collman, J. I. Brauman, T. R. Halbert, and K. S. Suslick, *Proc. Natl. Acad. Sci. U.S.A.*, **73**, 3333–3337 (1976).
(26) (a) C. H. Barlow, J. C. Maxwell, W. J. Wallace, and W. S. Caughey, *Biochem. Biophys. Res. Commun.*, **55**, 91–95 (1973); (b) J. C. Maxwell, J. A. Volpe, C. H. Barlow, and W. S. Caughey, *ibid.*, **58**, 166–171 (1974); (c) J. C. Maxwell and W. S. Caughey, *ibid.*, **60**, 1309–1314 (1974).
(27) A. M. Schaffer, M. Gouterman, and E. R. Davidson, *Theor. Chim. Acta*, **30**, 9–30 (1973).
(28) S. Aronowitz, M. Gouterman, and J. C. W. Chien, unpublished results.
(29) R. F. Kirchner and G. H. Loew, *J. Am. Chem. Soc.*, **99**, 4639–4647 (1977).
(30) (a) J. C. Norvell, A. C. Nunes, and B. P. Schoenborn, *Science*, **190**, 569–570 (1975); (b) E. J. Heidner, R. C. Ladner, and M. F. Perutz, *J. Mol. Biol.*, **104**, 707–722 (1976).
(31) M. Gouterman, L. K. Hanson, G.-E. Khalil, W. R. Leenstra, and J. W. Buchler, *J. Chem. Phys.*, **62**, 2343–2353 (1975).
(32) L. Pauling and C. D. Coryell, *Proc. Natl. Acad. Sci. U.S.A.*, **22**, 210–216 (1936).
(33) M. Cerdonio, A. Congiu-Castellano, F. Mogno, B. Pispisa, G. L. Romani, and S. Vitale, *Proc. Natl. Acad. Sci. U.S.A.*, **74**, 398–400 (1977).
(34) L. Pauling, *Proc. Natl. Acad. Sci. U.S.A.*, **74**, 2612–2613 (1977).
(35) (a) G. Lang and W. Marshall, *Proc. Phys. Soc., London*, **87**, 3–34, (1966); (b) H. Eicher and A. Trautwein, *J. Chem. Phys.*, **50**, 2540–2551 (1969); (c) N. Nakano, J. Otsuka, and A. Tasaki, *Biochim. Biophys. Acta*, **236**, 222–233 (1971); (d) *ibid.*, **278**, 355–371 (1972).
(36) (a) H. Eicher, D. Bade, and F. Parak, *J. Chem. Phys.*, **64**, 1446–1455 (1976); (b) B. H. Huynh, G. C. Papaefthymiou, C. S. Yen, J. L. Groves, and C. S. Wu, *ibid.*, **61**, 3750–3758 (1974).
(37) M. Zerner, Ph.D. Dissertation, Harvard University, 1966.
(38) J. Otsuka, *J. Phys. Soc. Jpn.*, **21**, 596–620 (1966).
(39) For a recent review of porphyrin π electron spectra see M. Gouterman, "The Porphyrins", Vol. III, Part A, D. Dolphin, Ed., Academic Press, New York, N.Y., in press, Chapter 1, and references cited therein.

(40) L. Vickery, T. Nozawa, and K. Sauer, J. Am. Chem. Soc., 98, 343-357 (1976).
(41) These equations were obtained from those given by P. J. Stephens, Annu. Rev. Phys. Chem., 25, 201-232 (1974).
(42) (a) P. J. Stephens, W. Suetaka, and P. N. Schatz, J. Chem. Phys., 44, 4592-4602 (1966); (b) A. J. McHugh, M. Gouterman, and C. Weiss, Theor. Chim. Acta, 24, 346-370 (1972).
(43) E. A. Dratz, Ph.D. Thesis, University of California, Berkeley, 1966.
(44) W. A. Goddard and B. D. Olafson, Proc. Natl. Acad. Sci. U.S., 72, 2335-2339 (1975).
(45) H. Eicher, private communication.
(46) It is theoretically possible, however, that the α and β hemes produce CD bands of opposite sign, resulting in cancellation of rotational strength.
(47) T. Nozawa, T. Yamamoto, and M. Hatano, Biochim. Biophys. Acta, 427, 28-37 (1976).
(48) D. A. Case, B. H. Huynh, and M. Karplus, J. Am. Chem. Soc., submitted.
(49) For CD spectra of deoxyhemoglobin in the visible-ultraviolet region see ref 19; for MCD spectra see ref 40 and 51; for single crystal spectra see ref 14 and J. Hofrichter, J. Mol. Biol., in press.
(50) As a consequence of this approximation, the $d_{xz} \rightarrow d_{x^2-y^2}$ and $d_{xz} \rightarrow d_{yz}$ transitions are artificially predicted to appear at zero frequency.
(51) J. I. Treu and J. J. Hopfield, J. Chem. Phys., 63, 613-623 (1975).
(52) B. H. Huynh, D. A. Case, and M. Karplus, J. Am. Chem. Soc., 99, 6103-6105 (1977).
(53) A. K. Chung and M. W. Makinen, J. Chem. Phys., 68, 1913-1925 (1978).

The Conformational Energy Surface of *trans,trans,trans*-1,5,9-Cyclododecatriene

Frank A. L. Anet* and T. N. Rawdah

Contribution No. 3959 from the Department of Chemistry, University of California, Los Angeles, California 90024. *Received February 10, 1978*

Abstract: ^1H and ^{13}C NMR spectra of *trans,trans,trans*-1,5,9-cyclododecatriene (**1**) have been measured from −5 to −180 °C. A dynamic NMR effect is observed in the ^1H spectra only, and this effect is associated with a conformational process which has a free energy of activation of 8.6 kcal/mol. These results are consistent with a single D_3 conformation for the triene. The conformational energy surface for ring inversion of the D_3 conformation to its mirror-image conformation has been investigated by iterative force-field calculations. The (strain energy) barrier of the best path for the ring inversion of the D_3 conformation is calculated to be 9.5 kcal/mol, in good agreement with the experimental (free energy) barrier. A systematic nomenclature is introduced in order to describe the conformations and transition states associated with the complex energy surface of **1**.

The trimerization of 1,3-butadiene by Ziegler-type catalysts provides an important source of 12-membered rings.[1,2] Under suitable conditions, *trans,trans,trans*-1,5,9-cyclododecatriene (**1**) is the predominant product, and it can be easily isolated in a pure state because of its relatively high melting point (34 °C). An x-ray diffraction structure of this isomer reveals a conformation with approximately D_3 symmetry;[3] a very similar structure has also been found in the Ni(0) complex[4] of this triene. The infrared and Raman spectra of **1** have been analyzed[5] in terms of a D_3 structure and valence force constants have been deduced for this molecule. Ermer and Lifson[6] have made use of the known conformation and vibrational frequencies of this triene to optimize force-field parameters which can be applied to unsaturated hydrocarbons in general. Dale and Greig[7] have observed a dynamic NMR effect in the methylene protons of **1** and have calculated a $\Delta G^{\ddagger}$ value of about 9 kcal/mol for site exchange of these protons. Dale has also briefly discussed conformational interconversions in **1**, and has pointed out that exchange of the methylene proton sites in the D_3 conformation requires a ring inversion to the mirror-image conformation.

In this paper, we investigate conformational interconversions in *trans,trans,trans*-1,5,9-cyclododecatriene by dynamic NMR and force field calculations.

Experimental Section

NMR spectra were obtained on a superconducting solenoid operating at 59 kG.[9,10] The proton spectra were obtained with standard 5-mm sample tubes in a frequency-sweep mode. The ^{13}C spectra are Fourier transforms of accumulated free induction decays and were obtained with 10-mm tubes under the following conditions: 45° pulse angle, 8K data points, 11-kHz spectrum width, and an exponential broadening function corresponding to 4 Hz broadening. A mixture of $CHCl_2F$-$CHClF_2$ (4:1) was used as a solvent, and a ^{19}F line of the solvent was employed for lock purposes. All temperatures were measured with a copper-constantan thermocouple situated in the probe a few centimeters below the sample.

Force-field calculations were carried out on an IBM-360/91 computer at the Campus Computer Network of UCLA, with a slightly modified version of Boyd's Molecular Builder IIA.[11]

Results and Discussion

NMR Data. ^{13}C NMR spectra of *trans,trans,trans*-1,5,9-cyclododecatriene were obtained from −5 to −180 °C. The allylic and vinylic carbon resonances occur at 32.9 and 132.7 ppm, respectively, at −12 °C, and these resonances show little chemical shift changes at lower temperatures. No dynamic NMR effect of any kind was observed. These results are in agreement with a single conformation of D_3 symmetry for the triene.

The ^1H NMR spectra of the all-trans triene showed a clear dynamic NMR effect at about −90 °C (Figure 1). The methylene proton resonance changes from a single line (δ 2.06) at −60 °C to two somewhat broad resonances (δ 1.90 and 2.26) at −138 °C. The coalescence temperature is −92 °C. Some fine structure is visible in the spectrum at −138 °C. Splittings due to spin-spin couplings should be very complex and are not expected to be well resolved. Since the chemical shift between the nonequivalent methylene protons is much larger (90 Hz) than any anticipated coupling constant, the rate constant at the coalescence temperature should be well approximated by the equation[12] $k = \pi\Delta\nu/\sqrt{2}$. Application of the absolute rate theory[13] with a transmission coefficient of 1 gives a free energy of activation ($\Delta G^{\ddagger}$) of 8.6 ± 0.2 kcal/mol at −92 °C.

The splitting of the methylene resonance into two equal intensity peaks at −138 °C and the lack of any splitting in the ethylenic proton resonance (δ 5.08) are in agreement with a D_3 conformation. Our ^1H NMR results are in reasonable agreement with the 60-MHz data of Dale and Greig,[7,8] who report a $\Delta G^{\ddagger}$ of about 9 kcal/mol.

0002-7863/78/1500-5003$01.00/0